

# Cu,Zn Superoxide Dismutase from *Photobacterium leiognathi* Is an Hyperefficient Enzyme<sup>†</sup>

Maria Elena Stroppolo,<sup>‡</sup> Marco Sette,<sup>§</sup> Peter O'Neill,<sup>||</sup> Francesca Polizio,<sup>‡</sup> Maria Teresa Cambria,<sup>⊥</sup> and Alessandro Desideri<sup>\*‡</sup>

INFM and Department of Biology, University of Rome "Tor Vergata", Rome, Italy; Department of Chemical Science and Technology, University of Rome "Tor Vergata", Rome, Italy; Radiation and Genome Stability Unit, Medical Research Council, Harwell, Didcot, Oxon OX11 0RD, U.K.; Institute of Biochemical and Pharmacological Sciences, University of Catania, Catania, Italy

Received March 12, 1998; Revised Manuscript Received June 24, 1998

**ABSTRACT:** The catalytic rate constant of recombinant *Photobacterium leiognathi* Cu,Zn superoxide dismutase has been determined as a function of pH by pulse radiolysis. At pH 7 and low ionic strength ( $I = 0.02$  M) the catalytic rate constant is  $8.5 \times 10^9 \text{ M}^{-1} \text{ s}^{-1}$ , more than two times the value found for all the native eukaryotic Cu,Zn superoxide dismutases investigated to date. Similarly, Brownian dynamics simulations indicate an enzyme–substrate association rate more than two times higher than that found for bovine Cu,Zn superoxide dismutase. Titration of the paramagnetic contribution to the water proton relaxation rate of the *P. leiognathi* with increasing concentration of halide ions with different radii indicates that the proteic channel delimiting the active site is wider than 4.4 Å. This is at variance with that found on the eukaryotic enzymes, and provides a rationale for the high catalytic rate of the bacterial enzyme. Evidence for solvent exposure of the active site different from that observed in the eukaryotic enzyme is suggested from the pH dependence of the water proton relaxation rate and of the EPR spectrum line shape, which indicate the occurrence of a prototropic equilibrium at pH 9.1 and 9.0, respectively. The pH dependence of the *P. leiognathi* catalytic rate has a trend different from that observed in the bovine enzyme, indicating that groups differently exposed to the solvent are involved in the modulation of the enzyme–substrate encounter.

Cu,Zn superoxide dismutases are a class of metalloenzymes that catalyze the dismutation of the superoxide anion into oxygen and hydrogen peroxide, thus protecting the cell from oxidative damage (*1*).<sup>1</sup> The eukaryotic Cu,Zn enzymes have been extensively investigated from both a structural (2, 3) and a functional point of view (4–7). The structure of the active site is highly conserved, and a similar catalytic rate value of about  $3 \times 10^9 \text{ M}^{-1} \text{ s}^{-1}$  is reported for all the eukaryotic species at neutral pH and low ionic strength ( $I = 0.02$ ) (6, 8, 9). This high value conflicts with the evidence that the catalytic copper site is only 0.1% of the enzyme

surface, and electrostatic facilitation has been proposed to explain such a high catalytic rate (10–13). Cu,Zn SODs actually represent the best example in which the catalytic event is diffusion-limited and in line, enzyme–substrate association rate calculated by Brownian dynamics simulation matches well the experimental catalytic rate in different SOD species and SOD derivatives (14, 15). Investigation of the pH dependence of the catalytic rate of the eukaryotic Cu,ZnSODs has indicated the occurrence of two pKs at around pH 9.3 (pK<sub>1</sub>) and 11.3 (pK<sub>2</sub>), respectively (6, 8, 9), which have been attributed to the conserved Lys120 and Lys134 (pK<sub>1</sub>) and to titration of the invariant Arg141, coupled to deprotonation of the copper-coordinated water molecule (pK<sub>2</sub>) (5, 6, 16, 17). In agreement, a transition of the EPR signal intensity (18) and of the water proton relaxation rate of the copper-bound water molecule (19) has been observed in the same pH range (11–11.5).

Much less is known on the structure–function relationship of the Cu,Zn bacterial SOD enzymes. A systematic investigation, including determination of the 3D structure and of the functional properties through the use of direct methods, of highly pure forms of bacterial SOD has only recently started. The 3D structure of PSOD (20) and *Escherichia coli* SOD (21) has been recently determined at high resolution. Both ESOD and PSOD preserve the eight stranded greek-key  $\beta$ -barrel folding characteristic of the eukaryotic Cu,Zn SODs (22); however, they are stable in a monomeric

<sup>†</sup>This work was partly supported by Italian National Research Council Project "Dinamica di proteine globulari" and by a MURST project "Struttura, Funzione ed Ingegneria di proteine globulari."

\* Author to whom correspondence should be addressed at Department of Biology, University of Rome "Tor Vergata", Via della Ricerca Scientifica e Tecnologica, 00133 Rome, Italy. Telephone: 39/0672594376. Fax: 39/0672594311. E-mail: [desideri@uniroma2.it](mailto:desideri@uniroma2.it).

<sup>‡</sup> INFM and Department of Biology, University of Rome "Tor Vergata".

<sup>§</sup> Department of Chemical Science, University of Rome "Tor Vergata".

<sup>||</sup> Radiation and Genome Stability Unit, Medical Research Council.

<sup>⊥</sup> Institute of Biochemical and Pharmacological Sciences, University of Catania.

<sup>1</sup> Abbreviations: BSOD, bovine Cu,Zn superoxide dismutase; 3D, three-dimensional; ESOD, *Escherichia coli* Cu,Zn superoxide dismutase; EDTA, ethylenediaminetetraacetic acid; EPR, electron paramagnetic resonance; FPLC, fast protein liquid chromatography; NMR, nuclear magnetic resonance; PSOD, *Photobacterium leiognathi* Cu,Zn superoxide dismutase.

and homodimeric form respectively (23–25). PSOD displays a novel dimer interface formed by  $\beta$ -strands 5e and 4f, not seen in the eukaryotic enzymes whose monomers interact through strands 1a and 8h (20). Differences at the level of the catalytic copper site between the prokaryotic and the eukaryotic enzymes have also been evidenced in solution through a spectroscopic investigation of the *Photobacterium leiognathi* (23) and the *Brucella abortus* enzyme (26). Due to deletion of part of the “electrostatic loop” (20), PSOD lacks residues Lys120, Glu130, Glu131, and Lys134, which are highly conserved in the eukaryotic enzymes and have been shown to be involved in the electrostatic attraction of the substrate (4–6).

These peculiar structural properties prompted us to investigate the dependence of the catalytic rate of PSOD on pH by pulse radiolysis, the only method which allows a direct determination of SOD activity. Moreover, the dimension and solvent exposure of the catalytic copper site has been investigated through EPR and water proton relaxation rate measurements. The enzyme is found to have an activity more than two times higher than that found in the eukaryotic enzymes, a finding that is correlated with the high accessibility of the channel delimiting the active site.

## MATERIALS AND METHODS

**Expression and Purification.** Recombinant PSOD has been expressed in *E. coli* and purified as previously described (23). Bovine SOD was prepared as previously described (27). Protein concentration was determined by the Lowry method (28). Copper content of the protein samples was determined by EPR spectroscopy using a  $\text{Cu}^{2+}$ -EDTA solution as a standard.

**EPR Spectroscopy.** EPR spectra were recorded at 300 and 100 K on a Bruker ESP300 spectrometer operating at 9.80 and 9.34 GHz, respectively, with 100 kHz field modulation. Protein copper concentration was 2 mM in 20 mM Tris-HCl at pH 7.5. The pH titration was carried out by adding small aliquots ( $\mu\text{L}$ ) of 1 M NaOH, and the pH was checked every time before and after each measurement with a pH meter using a microelectrode.

Best-fit of the EPR pH dependence was carried out by the steepest descent method, using the following equation to simulate one prototropic equilibrium:

$$I = I_{\max}([H^+]/(K + [H^+])) \quad (1)$$

where  $I$  is the EPR signal intensity,  $I_{\max}$  the EPR signal intensity at neutral pH, and  $K$  the equilibrium dissociation constant. The same equation was also used to fit the pH dependence of the water proton relaxation rate data.

**NMR Spectroscopy.** The water proton relaxation rate of Cu,Zn PSOD as a function of pH in the range 7.0–11.5 was determined using a MiniSpec P20 working at 20 MHz and at 20 °C.  $T_1$ s were obtained using an inversion–recovery pulse sequence,  $180^\circ\text{-}\tau\text{-}90^\circ$ , where the angles represent the extent of rotation of water magnetization and  $\tau$  is variable delay. Thirty four different experiments ( $\tau$  values) were recorded to well evaluate  $T_1$ . The standard deviation was always lower than 5%. The protein copper concentration was 1 mM in 20 mM Tris-HCl at pH 7.0. The titration was carried out using the same method as for the EPR spectra. Data were converted to molar water proton relaxation rate

using the expression given by Terenzi et al. (19), i.e., by subtracting the diamagnetic water contribution and normalizing to 1 mM of copper. Dissociation constants for the halide anions were determined by using the following equation, which is valid under the assumption of low-affinity binding (29):

$$R = ((K_d/(K_d + L_o)) (R_f - R_b) + R_b) \quad (2)$$

where  $R$  is the observed water proton relaxation rate,  $K_d$  is the dissociation constant,  $L_o$  is the molar concentration of ligand, and  $R_f$  and  $R_b$  represent the water proton relaxation rate in the absence and presence of saturating amount of ligand, respectively. In this equation, the molar fraction of the free enzyme, i.e., the molar fraction of enzyme containing water in the active site, is represented by  $K_d/(K_d + L_o)$ .

**Activity Assays.** Activity assays were carried out by the pulse radiolysis method (8, 30), based on the dependence of the first-order rate of loss of  $\text{O}_2^-$ , monitored spectrophotometrically at 250 nm (31), on the SOD concentration. To avoid binding of anions such as phosphate, chloride, or formate that are known to directly interact with the active site and to perturb the activity (31–34), the enzyme was assayed in Tris-MES, up to pH 7.20, Tris-Mops buffer in the pH range 7.0–9.0, and in borate from pH 9 and above. In all cases, the assay mixture contained 0.1 M ethanol and 0.1 mM EDTA, and the buffer concentrations were varied between 0.01 and 0.03 M in order to keep the ionic strength constant to  $I = 0.02$  M. The concentration of ethanol was chosen to ensure the majority of the OH radicals to interact with ethanol which within the pulse duration interacts with oxygen. It is well documented that  $\alpha$ -hydroxyl radicals give superoxide and that alcohol peroxy radicals do not interact with SOD (35).

Solutions contained in a 0.7 cm path length optical cell were irradiated with a 1.6  $\mu\text{s}$  electron pulse giving  $[\text{O}_2^-] = 15 \mu\text{M}$ . The concentration of the superoxide was determined from the absorbance at 250 nm, assuming extinction coefficient  $\epsilon_{250} = 2000 \text{ M}^{-1} \text{ cm}^{-1}$  (36). Since protein concentration for each sample varied in the range 0.2–1.0  $\mu\text{M}$ , the activity assays were carried out with  $[\text{O}_2^-] \gg [\text{SOD}]$ , i.e., under turnover conditions. The reaction of superoxide with hydrogen dioxide is taken into account in the determination of the second-order rate constant for interaction of superoxide with PSOD that was determined from measurements of the first-order rate of loss of superoxide at three different enzyme concentrations. The error of first-order rate constant at a given enzyme concentration was obtained from at least three different determinations and is at the most  $\pm 10\%$ . The enzyme concentration used was changed within the range stated in order to compensate for the lower activity at higher pH values.

Best fit of the rate pH dependence was carried out by the steepest descent method, using the following equation to simulate three pKs prototropic equilibria respectively:

$$A = A_{\max}((A_1[H^+]/(K_1 + [H^+])) + (A_2[H^+]/(K_2 + [H^+])) + (A_3[H^+]/(K_3 + [H^+]))) \quad (3)$$

where  $A$  is the catalytic activity of the enzyme,  $A_{\max}$  is the catalytic constant at neutral pH,  $K_1$ ,  $K_2$ , and  $K_3$  are the

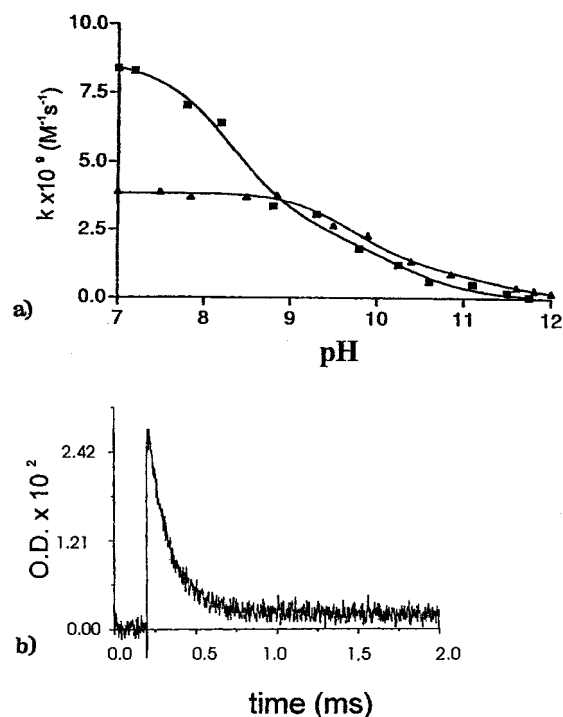


FIGURE 1: (a) pH dependence of the catalytic activity of the PSOD (■) and bovine SOD (▲) determined by pulse radiolysis. Continuous line represents the best fit of the experimental data using eq 3. The assays for both enzymes were carried out at 20 °C and at 20 mM ionic strength. The protein concentration for each sample varied in the range 0.2–1.0 mM. For further details, see Materials and Methods. (b) Typical time dependence for the loss of optical absorbance of superoxide in the presence of 0.9 mM PSOD at pH 7.0.

equilibrium dissociation constants, and  $A_1$ ,  $A_2$ , and  $A_3$  are the relative contributions of each pK to the activity curve.

**Brownian Dynamics Calculations.** Brownian dynamics simulations of the diffusion of superoxide under the influence of the protein-generated electrostatic field were carried out on a Silicon Graphics O<sub>2</sub> R5000 with a modification of a previously described method (14, 37). The simulation method and parameters have been described in detail elsewhere (15). Electrostatic potential was calculated with the program DelPhi (Biosym, Inc.) using the focusing procedure (38). Trajectories (10 000) were run for each simulation; values of 4 and 78.5 have been assigned to the dielectric constant of protein interior and solvent respectively (39). The ion exclusion radius (38) was set to 2 Å. 3D coordinates of PSOD native structure, kindly provided by Prof. M. Bolognesi, were used to simulate enzyme–substrate encounter.

## RESULTS AND DISCUSSION

**Determination of the Catalytic and of the Enzyme–Substrate Association Rate.** Figure 1a shows the pH dependence of the catalytic rate of PSOD at 0.02 M ionic strength in the pH range 7–12 compared to that of the bovine enzyme measured in the same condition. The second-order rate constant for the interaction of Cu,Zn SOD with superoxide was determined from the dependence of the first-order rate of decay of  $\text{O}_2^-$  on Cu,Zn SOD concentration under turnover conditions. A typical time dependence of the loss of the optical absorbance of superoxide in the presence of

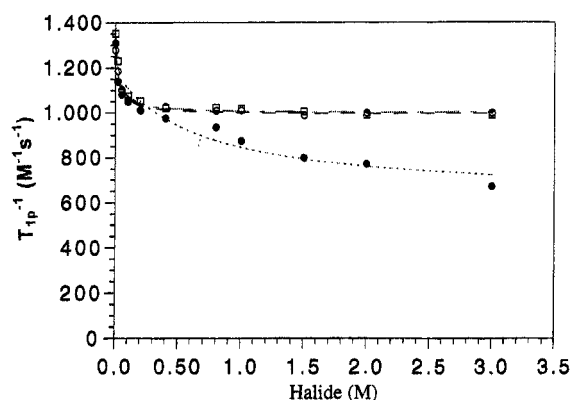


FIGURE 2: Molar water proton relaxation rate ( $T_{1p} - 1$ ) of Cu,Zn PSOD in the presence of increasing amounts of halide ions:  $\text{Br}^-$  (□),  $\text{Cl}^-$  (○),  $\text{I}^-$  (●). The spectra were recorded in 20 mM Tris-HCl at pH 7.0 and at 20 °C. Copper concentration was 1 mM. The lines represent the fit of the experimental data by using eq 2 reported in Materials and Methods.  $\text{Br}^-$  (—);  $\text{Cl}^-$  (---);  $\text{I}^-$  (···).

0.9  $\mu\text{M}$  PSOD is reported in Figure 1b, to show the signal-to-noise ratio of the data. At pH values higher than 9.0, *P. leiognathi* and bovine SOD display a similar, although not identical, catalytic rate, while at pH 7 PSOD has a rate of  $8.5 \pm 0.8 \times 10^9 \text{ M}^{-1} \text{ s}^{-1}$ , a value more than twice that found in the bovine and all native eukaryotic enzymes under the same conditions (8). It is interesting to notice that native PSOD displays the highest catalytic rate ever reported for any SOD enzyme, higher than that measured in the eukaryotic mutants engineered to have a facilitated diffusion rate of the substrate toward the active site (4, 5).

Brownian dynamics simulations carried out considering 10 000 trajectories of incoming substrate under the influence of Brownian motion and of the enzyme electrostatic field indicated that the PSOD to BSOD enzyme–substrate association rate ratio is 2.6. It is likely that the new dimer assembly shown to occur in the bacterial enzyme (20) produces a new charge distribution coupled with some local structural changes at the level of the active site (23) which may help the diffusion of the superoxide toward the catalytic metal center.

**Relaxometric Titration with Anions.** To verify if the facilitated diffusion of the substrate toward the active site could be due to an increase of the dimension of the channel delimiting the active site, the water proton relaxation rate of aqueous solution of superoxide dismutase at different concentration of halide anions having different atomic radius, i.e.,  $\text{Cl}^-$  ( $r = 1.81 \text{ Å}$ ),  $\text{Br}^-$  ( $r = 1.87 \text{ Å}$ ), and  $\text{I}^-$  ( $r = 2.20 \text{ Å}$ ), have been measured at pH 7.0. Figure 2 shows that, although to differing extents, the water proton relaxation rate value is reduced upon increasing halide concentration. Reduction of water proton relaxation rate values of aqueous solution containing superoxide dismutase has been explained in the eukaryotic Cu,Zn SOD to be due to the removal of the water molecule coordinated to the copper atom by the anion. Further, it has been used to determine the affinity constant of the anions for that binding site and to evaluate the dimension of the active site channel (34). The data of Figure 2 indicate that  $\text{Cl}^-$  and  $\text{Br}^-$ , although not being able to completely quench the water proton relaxation rate value, bind to the copper site; on the other hand,  $\text{I}^-$  almost completely abolishes the starting water proton relaxation rate value of the enzyme at high  $\text{I}^-$  concentration. In the case



Table 1: Dissociation Constant of the Halide Anions for *P. leiognathi* Cu,Zn SOD Evaluated from Water Proton Relaxation Rate Measurements

| anion           | atomic radius (Å) | $K_d$ (M) <i>P. leiognathi</i> Cu,ZnSOD |
|-----------------|-------------------|---|
| Cl <sup>-</sup> | 1.81              | 0.029                                   |
| Br <sup>-</sup> | 1.87              | 0.026                                   |
| I <sup>-</sup>  | 2.20              | 0.250                                   |

of iodide we checked that copper was not reduced by iodide by monitoring the presence of the absorbance band at 680 nm typical of the copper in the oxidized state (40).

Previous water proton relaxation rate and activity titration on bovine SOD indicated that Br<sup>-</sup> and Cl<sup>-</sup> were able to reach the active site, although being able to only partially quench the water proton relaxation rate value (34). On the other hand, I<sup>-</sup> was not able to perturb the water proton relaxation rate value of the bovine enzyme, providing convincing evidence that the dimension of the active site channel is less than the atomic diameter of I<sup>-</sup> (34). In the case of PSOD the accessibility of the copper ion to I<sup>-</sup> implies that the width of the active site channel in PSOD is larger than in the eukaryotic SODs, i.e., larger than 4.4 Å.

The lower extent of the water proton relaxation rate reduction produced by Br<sup>-</sup> and Cl<sup>-</sup> with respect to I<sup>-</sup> can be related to differences in the dimensions of the anions. In fact, the residual water proton relaxation rate value observed with Cl<sup>-</sup> and Br<sup>-</sup> may be explained in terms of the small radius of the two anions, which allows a water molecule to stay in the proximity of the paramagnetic copper while the larger I<sup>-</sup>, at saturating anion concentrations, almost completely removes it. The fit of the experimental data, obtained by using eq 2 reported in Materials and Methods, is also displayed in Figure 2. Such a fit allows us to determine the dissociation constants, which in the case of Cl<sup>-</sup> and Br<sup>-</sup> is 1 order of magnitude lower than that displayed for I<sup>-</sup> (Table 1). Moreover, the bacterial enzyme displays a dissociation constant for Cl<sup>-</sup> and Br<sup>-</sup> which is 1 order of magnitude lower than that found in the eukaryotic enzyme (34). Such values are consistent with an active site channel having a larger width in PSOD than in the eukaryotic enzymes (34). The large dimension of the active site of *P. leiognathi* can be correlated with its high catalytic rate since increasing the accessibility of the active site increases the enzyme–substrate association rate.

**pH Dependence of the Proton Water Proton Relaxation Rate and of the EPR Spectra.** The pH dependence of the proton water proton relaxation rate of PSOD is reported in Figure 3. The value at neutral pH is lower than that observed in the eukaryotic enzymes (19, 34), indicating a different coordination (i.e., a slightly longer Cu–H<sub>2</sub>O distance) of the copper-bound water molecule. Moreover the pH dependence indicates the occurrence of a prototropic equilibrium with  $pK = 9.1$ , diagnostic of a local rearrangement around the copper site. In eukaryotic Cu,Zn SODs, such equilibrium occurs with  $pK = 11.2$  and has been attributed to deprotonation of the copper-coordinated water molecule (19). The same interpretation may apply for PSOD, and the occurrence of a  $pK$  about two units of pH lower than that observed in eukaryotic SODs indicates a different degree of exposure of the metal site to the external water solvent in line with the

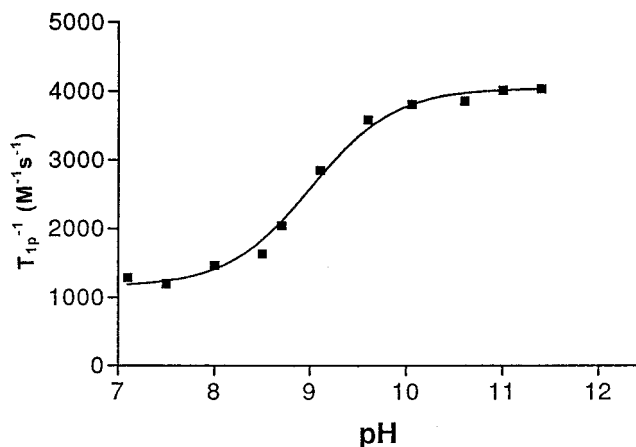


FIGURE 3: Molar water proton relaxation rate ( $T_{1p} - 1$ ) of Cu,Zn PSOD in 20 mM Tris-HCl in the pH range 7.0–11.5, at 20 °C. Copper concentration was 1 mM.

information on the active site accessibility determined from the halide titration experiments.

In a previous study (23), we have shown that the low-temperature EPR spectrum of PSOD undergoes a transition from a rhombic to an axial shape, governed by an apparent  $pK = 9.9$  (23). Since such a value is 0.8 unit of pH higher than the  $pK$  value observed in the proton relaxation measurements reported in Figure 3, the EPR spectra of the copper active metal of PSOD have been measured as a function of pH at room temperature, i.e., at the same temperature of the proton relaxation measurements. The spectra undergo a reversible transition up to pH 11.5, while at higher pH an irreversible biuret-type species is observed. The spectra, reported in Figure 4, display two distinct differences when compared to those recently reported at low temperature (23).

(1) The line shape of the spectrum is dependent on the state of the protein (i.e., frozen or solution state), as can be seen more readily in Figure 5, where the low- and room-temperature EPR spectra of the protein at pH 7 are reported on a  $g$  scale to allow direct comparison. In particular, it can be seen that the fourth copper parallel hyperfine line collapses into the perpendicular region at low temperature (23) while it is readily discernible at room temperature.

(2) The  $pK$  monitored at room temperature by the rhombic-to-axial transition occurs at pH 9.0 (see Figure 4, top) instead of pH = 9.9 as previously reported for the low-temperature spectra (23).

Modification of the EPR line shape, depending on the state of the protein, is a novel finding, since eukaryotic Cu,Zn SODs are known to have an identical EPR spectrum at both room and liquid nitrogen temperatures (41, 42). This modification may be taken as a further indication of a slight geometrical rearrangements of the ligands surrounding the metal site in the prokaryotic as compared with that of the eukaryotic enzymes (23). In particular we can infer that the seven residues insertion in the S-S loop have conferred a high flexibility which may provide different conformations in the prokaryotic Cu,Zn SOD depending on temperature (20). It is interesting to notice that the  $pK$  evaluated from the room-temperature EPR spectra is identical, within the experimental error, to that obtained from the water proton relaxation rate measurement, suggesting that the two techniques monitor the same phenomenon, i.e., deprotonation of the copper-coordinated water molecule.

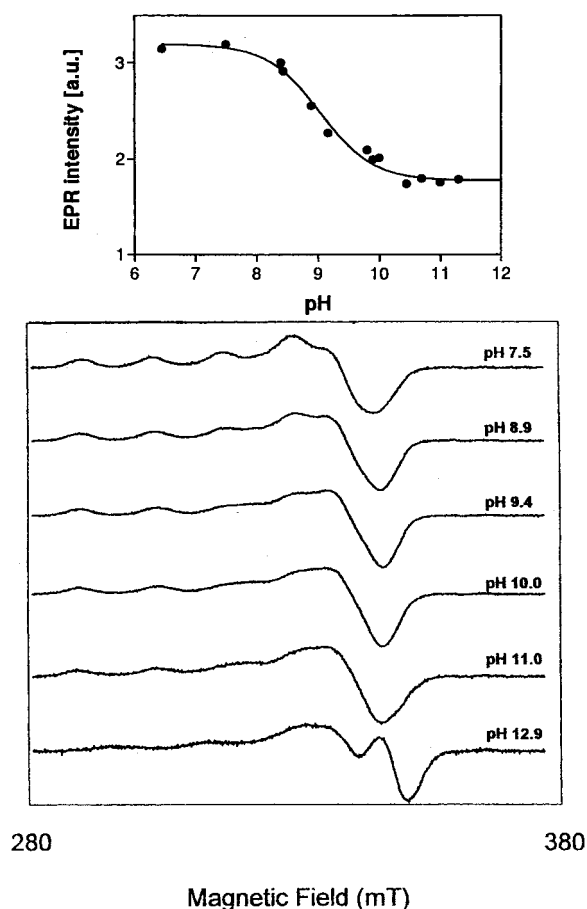


FIGURE 4: Bottom: EPR spectra of 2 mM *P. leiognathi* Cu,Zn SOD, in 20 mM Tris HCl as function of pH: pH 7.50; 8.90; 9.40; 10.0; 11.0; 12.9. Spectral conditions: 20 mW, microwave power; 9.80 GHz, microwave frequency; 1.0 mT, modulation amplitude; temperature 20 °C. Top: dependence on pH of the difference in intensity of the third parallel hyperfine lines at 317 mT, reported in arbitrary units.

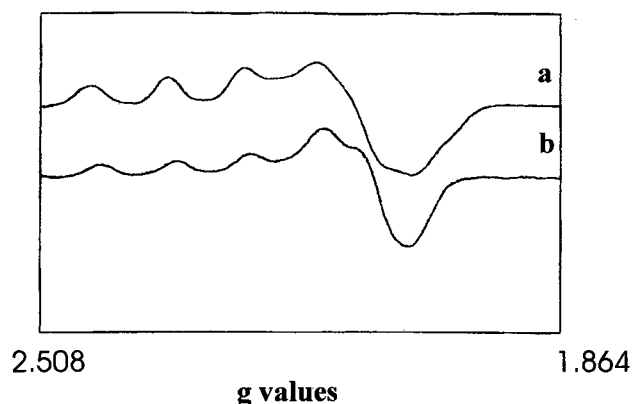


FIGURE 5: EPR spectra of PSOD in the frozen state (a), and at room temperature (b). The spectra are reported on a g scale to allow a direct comparison of their shape.

**pH Dependence of the Catalytic Rate.** The pH dependence of the catalytic rate reported in Figure 1 for the *P. leiognathi* enzyme has a trend different from the one observed in the bovine enzyme. In particular, the catalytic rate of the bovine enzyme is constant from pH 7 to 9, and a reversible decrease of the activity is observed only at pH higher than 9. Previous fit of the catalytic rate pH dependence of the bovine or other eukaryotic SOD enzymes indicated the presence of two pK

values, the first one at pH 9.0–9.5 and the second one at 11.0–11.3 (6, 8). In the case of *P. leiognathi* SOD the best fit of the experimental line is obtained by considering three different prototropic equilibria with  $pK_1 = 8.3$ ,  $pK_2 = 9.3$ , and  $pK_3 = 10.4$ . Such a fit must be considered only indicative because of the sparseness of the data and the inherent error of the catalytic activity up to 10%. However, the decrease of the catalytic rate as soon as the pH deviates from 7.0 and the different shape of the pH dependence of the two curves of Figure 1 indicate that the enzyme–substrate encounter in *P. leiognathi* SOD is governed by groups surrounding the active site differently exposed to the solvent with respect to those involved in the eukaryotic enzymes.

## CONCLUSION

In this study we have shown that Cu,Zn SOD from *P. leiognathi* displays structural and functional features distinct from those observed in the eukaryotic Cu,Zn SODs. In particular:

- (1) PSOD displays at neutral pH the highest catalytic rate ever measured in any Cu,Zn SOD (i.e., more than twice that found in the native Cu,Zn SODs from eukaryotic species).
- (2) The width of the channel limiting the access to the copper active site is wider than that found in the eukaryotic enzymes, measuring more than 4.4 Å.
- (3) Deprotonation of the copper-coordinated water molecule occurs with  $pK \sim 9.1$ , at least two pH units lower than that observed in the eukaryotic enzyme.
- (4) The pH dependence of the catalytic rate is different from that of the eukaryotic enzyme, indicating that it is influenced by deprotonation of differently located and solvent-exposed groups.

These results pose interesting questions on the biological relevance of the presence of Cu,Zn SOD in the periplasm of bacteria and point out the usefulness of bacterial SODs to obtain a deeper understanding of the function of this class of enzymes.

## ACKNOWLEDGMENT

We express our gratitude to Prof. M. Paci and Dr. Mauro Fasano for helpful suggestions concerning the relaxivity measurements.

## REFERENCES

1. Bannister, J. V., Bannister, W. H., and Rotilio, G. (1987) *Crit. Rev. Biochem.* 22, 111–180.
2. Tainer, J. A., Getzoff, E. D., Beem, K. M., Richardson, J. S., and Richardson, D. C. (1982) *J. Mol. Biol.* 160, 181–217.
3. Djinovic-Carugo, K., Battistoni, A., Carri', M. T., Polticelli, F., Desideri, A., Rotilio, G., Wilson, K. S., and Bolognesi, M. (1996) *Acta Crystallogr. D52*, 176–188.
4. Getzoff, E. D., Cabelli, D. E., Fisher, C. L., Parge, H. E., Viezzoli, M. S., Banci, L., and Hallewell, R. A. (1992) *Nature* 358, 347–351.
5. Polticelli, F., Bottaro, G., Battistoni, A., Carri', M. T., Djinovic-Carugo, K., Bolognesi, M., O'Neill, P., Rotilio, G., and Desideri, A. (1995) *Biochemistry* 34, 6043–6049.
6. Polticelli, F., Battistoni, A., O'Neill, P., Rotilio, P., and Desideri, A. (1996) *Protein Sci.* 5, 248–253.
7. Fisher, C. L., Cabelli, D. E., Hallewell, R. A., Beroza, P., Lo, T. P., Getzoff, E. D., and Tainer, J. A. (1997) *Proteins* 29, 103–112.

8. O'Neill, P., Davies, S., Fielden, M., Calabrese, L., Capo, C., Marmocchi, F., Natoli, G., and Rotilio, G. (1988) *Biochem. J.* 251, 41–46.
9. Polticelli, F., O'Neill, P., Costanzo, S., Lania, A., Rotilio, G., and Desideri, A. (1995) *Arch. Biochem. Biophys.* 321, 123–126.
10. Koppenol, W. H. (1981) *Oxygen and Oxy-Radicals in Chemistry and Biology* (Rodger, M. A. J., and Powers, E. L., Eds.) pp 671–674, Academic Press, New York.
11. Getzoff, E. D., Tainer, J. A., Weiner, P. K., Kollman, P. A., Richardson, J. S., and Richardson, D. C. (1983) *Nature* 306, 287–290.
12. Klapper, L., Hagstrom, R., Fine, R., Sharp, K., and Honig, B. (1986) *Proteins: Struct., Funct., Genet.* 1, 47–59.
13. Desideri, A., Falconi, M., Polticelli, F., Bolognesi, M., Djinozovich, K., and Rotilio, G. (1992) *J. Mol. Biol.* 223, 337–342.
14. Sines, J. J., Allison, S. A., and McCammon, J. A. (1990) *Biochemistry* 29, 9403–9412.
15. Sergi, A., Ferrario, M., Polticelli, F., O'Neill, P., and Desideri, A. (1994) *J. Phys. Chem.* 98, 10554–10557.
16. Polticelli, F., Battistoni, A., Bottaro, G., Carri', M. T., O'Neill, P., Desideri, A., and Rotilio, G. (1994) *FEBS Lett.* 352, 76–78.
17. Fisher, C. L., Cabelli, D. E., Tainer, J. A., Hallewell, R. A., and Getzoff, E. D. (1994) *Proteins* 19, 24–34.
18. Calabrese, L., Polticelli, F., Capo, C., and Musci, G. (1991) *Free Radical Res. Commun.* 12–13, 305–312.
19. Terenzi, M., Rigo, A., Franconi, C., Mondovi', B., Calabrese, L., and Rotilio, G. (1974) *Biochim. Biophys. Acta* 351, 230–236.
20. Bourne, Y., Redford, S. M., Steinman, H. M., Lepock, J. R., Tainer, J. A., and Getzoff, E. D. (1996) *Proc. Natl. Acad. Sci. U.S.A.* 93, 12774–12779.
21. Pesce, A., Capasso, C., Battistoni, A., Folcarelli, S., Rotilio, G., Desideri, A., and Bolognesi, M. (1997) *J. Mol. Biol.* 274, 408–420.
22. Bordo, D., Djinozovich, K., and Bolognesi, M. (1994) *J. Mol. Biol.* 238, 366–386.
23. Foti, D., Lo Curto, B., and Cuzzocrea, G., Stroppolo, M. E., Polizio, F., Venanzi, M., and Desideri, A. (1997) *Biochemistry* 36 (23), 7109–7113.
24. Benov, L., Sage, H., and Fridovich, I. (1997) *Arch. Biochem. Biophys.* 340, 305–310.
25. Battistoni, A., Folcarelli, S., Cervoni, L., Polizio, F., Desideri, A., Giartosio, A., and Rotilio, G. (1998) *J. Biol. Chem.* 273, 5655–5661.
26. Chen, Y. L., Park, S., Thornburg, R. W., Tabatabai, L. B., and Kintanar, A. (1995) *Biochemistry* 34, 12265–12275.
27. McCord, J., and Fridovich, I. (1969) *J. Biol. Chem.* 244, 6049–6055.
28. Lowry, O. H., Rosebrough, N. J., Farr, A. R., and Randall, R. J. (1951) *J. Biol. Chem.* 193, 265–275.
29. Bertini, I., and Luchinat, C. (1996) *Coord. Chem. Rev.* 150, 111–130.
30. O'Neill, P., and Chapman, P. W. (1985) *Int. J. Radiat. Biol.* 47, 71–80.
31. Fielden, E. M., Roberts, P. B., Bray, R., Lowe, D., Mautner, G., Rotilio, G., and Calabrese, L. (1974) *Biochem. J.* 139, 49.
32. Mota de Freitas, D., and Valentine, J. S. (1984) *Biochemistry* 23, 2079–2082.
33. Sette, M., Paci, M., Desideri, A., and Rotilio, G. (1992) *Biochemistry* 31, 12410–12415.
34. Rigo, A., Stevanato, R., Viglino, P., and Rotilio, G. (1977) *Biochem. Biophys. Res. Commun.* 79, 776–783.
35. O'Neill, P., and Fielden, E. M. (1980) *Development in Biochemistry* (Bannister, J. V., and Hill, H. A. O., Eds.) pp 357–363, Elsevier, Holland.
36. Rabani, J., and Nielson, S. O. (1969) *J. Phys. Chem.* 73, 3736–3744.
37. Sharp, K., Fine, R., and Honig, B. (1987) *Science* 236, 1460–1463.
38. Gilson, M. K., Sharp, K. A., and Honig, B. H. (1987). *J. Comput. Chem.* 9, 327–335.
39. Gilson, M., and Honig, B. (1988) *Proteins* 4, 7–18.
40. Cupane, A., Leone, M., Militello, V., Stroppolo, M. E., Polticelli, F., and Desideri, A. (1995) *Biochemistry* 34, 16313–16319.
41. Bertini, I., Borghi, E., Luchinat, C., and Scozzafava, A. (1981) *J. Am. Chem. Soc.* 103, 7779–7783.
42. Paci, M., Desideri, A., Sette, M., and Rotilio, G. (1991) *Arch. Biochem. Biophys.* 286, 222–225.

BI980563B